

**IDETC2016-59643**

## DEVELOPMENT OF AUTONOMOUS ROBOTIC CATARACT SURGERY DEVICE

**Matthew Francom**  
Virginia Tech  
Blacksburg, VA, USA

**Clinton Burns**  
Virginia Tech  
Blacksburg, VA, USA

**Philip Repisky**  
Virginia Tech  
Blacksburg, VA, USA

**Benjamin Medina**  
Virginia Tech  
Blacksburg, VA, USA

**Alex Kinney**  
Virginia Tech  
Blacksburg, VA, USA

**Erick Tello**  
Virginia Tech  
Blacksburg, VA, USA

**Pinhas Ben-Tzvi**  
Virginia Tech  
Blacksburg, VA, USA  
[bentzvi@vt.edu](mailto:bentzvi@vt.edu)

### ABSTRACT

The current rate of incidence of cataracts is increasing faster than treatment capacity, and an autonomous robotic system is proposed to mitigate this by carrying out cataract surgeries. The robot is composed of a three actuator RPS parallel mechanism in series with an actuated rail mounted roller that moves around the eye, and is designed to perform a simplified version of the extracapsular cataract surgery procedure autonomously. The majority of the design work has been completed, and it is projected that the system will have a tool accuracy of 0.167 mm, 0.141 mm, and 0.290 mm in the x, y, and z directions, respectively. Such accuracies are within the acceptable errors of 1.77mm in the x and y directions of the horizontal plane, as well as 1.139 mm in the vertical z direction. Tracking of the tool when moving at 2 mm/s should give increments of 0.08 mm per frame, ensuring constant visual feedback. Future work will involve completing construction and testing of the device, as well as adding the capability to perform a more comprehensive surgical procedure if time allows.

### I. INTRODUCTION

#### A. Cataracts

Despite advances in medicine, the only way to counteract the prevalence of cataract-induced blindness is through surgery; it is estimated that 3,000 operations per million people per year are required to meet current demand in Southeast Asia, and 2,000 per year in Africa. While India has reached levels

approaching this, other Southeast Asian states generally do not see rates of surgery above 1,500 per year per million people, and African countries do not reach even 500 [1]. Although demand for cataract surgery is high, cost barriers and lack of qualified surgeons prohibit patients from receiving adequate care [1,2].

Broadly, cataracts are a clouding of the eye's lens, preventing light from focusing and reaching the retina and are cause for over 40% of all blindness worldwide [3, 4]. While there are many causes from aging, sunlight, steroids, etc., the process for removing them relies on two methods: intracapsular and extracapsular extraction [4]. Most surgeries in the developing world make use of the extracapsular extraction method using small incision cataract surgery for its comparative affordability and simplicity [4]. Under such a procedure, the entire lens is removed intact while intracapsular requires a phacoemulsification probe to break up and vacuum the fragments while inside the eye.

#### B. History of Medical Robotics

Thrusts for bringing robotics into surgery can already be seen in units such as the da Vinci robot from Intuitive Surgical® for general laparoscopic surgery controlled by a surgeon [6]. Benefits from its use have been numerous, including hand tremor reduction from surgeons, minimal incisions, and decrease hospital stays. At \$1.5M per unit, cost prohibits many healthcare settings from adopting the da Vinci robot. Additionally, extensive user training has limited larger scale deployment of the technology. [5, 6].

More recent endeavors include the Raven II, which has provided an open-source platform for attempting tele-operated and even autonomous surgical removal of objects within a work area [7]. Using a stereo vision system in conjunction with a multilateral manipulation, surgical debridement was carried out on 120 fragments, with speed and false positives recorded against a human operator. Despite taking nearly three times longer than the human operator, only 7.0% of pieces were classified as grasp failures. Preliminary issues with completing the procedure included uncertainty in state estimation resulting from slack in cables and uncertainty in the vision system. These issues were alleviated through background subtraction and tool markings. [7]

Use of autonomy in surgical applications has thus far been confined to research into tasks directed by a surgeon, such as tool holding, knot typing, needle passing, or suturing. However, planning a path through soft tissue with obstructions requires constant feasibility assessment during most surgeries, providing an array of technical hurdles. Johns Hopkins University has made significant strides towards this goal by classifying motion data from the da Vinci. Using a Hidden Markov Model, the researchers were able to successfully identify 92% of surgical gestures in suturing. [8]. Optical flow monitoring has also been examined for training models through motion primitives. Despite some success, 30% of breakpoints are manually set and computing time requires up to 16.5 minutes, making it still far from implementation [9].

Specifically for ocular surgery, the IRISS robotic surgical platform has been able to carry out intraocular surgery on ex vivo porcine eyes, under a master-slave configuration [10]. Use of the IRISS led to the first system to perform a successful curvilinear capsulorhexis as well as an entire cataract surgery. However, the lack of a tracking for eye movement in a live patient prevents further testing. Incorporation with a femtosecond laser has been mentioned, but implementation has not been pursued due to high costs and difficult learning curves for surgeons [10].

Modifications of existing technology have been in development for ocular procedures for years, such as an affordable YAG laser for posterior capsule opacification procedures [11]. Through the femtosecond laser, automation has already become part of the surgical procedure in some American surgery centers. Confined to only the surgical components of entry incision, capsulorhexis, and fragmentation of the cataract, it performs within the tolerances expected of human surgeon.

In this paper, we propose the development of an autonomous system built specifically to perform cataract surgery in order to help meet the worldwide demand. The platform proposed in this paper aims to specialize in only extracapsular cataract surgery, which we believe will allow for a simplified, affordable, and more easily produced system than existing surgical robots. Paper organization follows as such: Section II sets the project expectations and minimum requirements for carrying out the procedure. Section III delves into the specifications of the models and uncertainties in control

when the unit is constructed. Section IV provides the conclusions of the work thus far and the direction of future work implementing the platform.

## II. SURGERY SYSTEM FRAMEWORK

### A. Project Expectations

Communication with Dr. John Wood, MD, an ophthalmologist in Salem, VA with international work experience in Latin America performing cataract surgery, has confirmed the magnitude of cases found in developing nations. While his local surgeries employ phacoemulsification probes for intracapsular extraction, his knowledge extends to the work performed in India and areas where extracapsular procedures are common.

At his invitation, the team was able to observe six surgeries, both completely manual and assisted by the femtosecond laser machine. Insights from the operations and follow up with patients allowed for an informed decision when deciding on the scope of the prototype system. Replicating his procedure would require two surgical manipulators with 7 degrees of freedom and precision of 0.5 mm about a remote center of motion (RCM) about the surface of the incision. In addition, monitoring of the eye for pressurization loss and the injection and vacuuming of three viscoelastic gels would require pressure sensing capabilities in the eye or stereo vision to monitor deflation. Use of the phaco probe would also constitute a large portion of the budget adding further design constraints.

The scope of the project includes only surgical operations and does not involve pre-operational or post-operational procedures. Pupil dilation and local anesthetic to the eye would require actuation for controlled fluid injection, while tool changing and bandaging require entirely separate mechanisms from those actually entering the eye.

Surgery expectations for the platform minimum viable product for the device deviate from the full surgery significantly due to the need to maintain a one year development period and a budget of roughly \$3,300. While the normal surgery requires a workspace of 36.5 mm, 31.4 mm, and 20.6 mm in the x, y, and z-planes and minimum angular freedom of 116 ° and 106° in the x and y-planes [12], our system lacks the z-plane motion and y-planes angulation.

### B. Surgery Goals

Only a simplified version of the extracapsular cataract surgery is expected to be carried out autonomously. More specifically, the system must be able to create a flat, 2-D scleral tunnel, remove the existing lens within the eye, and replace it with a synthetic version. This simplified procedure will operate almost exclusively in one plane of motion, although the system is built to allow vertical motion for future expansions on this work. Additionally, the system has the physical capability to perform a capsulorhexis, as well as more complicated scleral tunnel incisions often used in similar surgeries. While not

considered necessary for the minimum viable product, these will be implemented if project time and budget allow.

In addition, the availability of ex vivo animal eyes with cataracts proves a limiting factor in testing with the manipulation and vision detection system. Placeholder material and patterns to match organic shear moduli and physiological construction will be utilized instead. Main testing will be on puncture force requirements and visual similarity to an adult human eye.

### III. Device System

#### A. Overview of the System Design

A kinematic, workspace, and uncertainty model of the system has been developed for performing the above procedure. The CAD model of the system is seen in Figures 1 and 2. Setting the tools' global positioning, the curvilinear rail seen is able to rotate the entire assembly about the eye and perform the entry incision. In order to perform the simplified procedure, we employ a three degree of freedom revolute-parallel-spherical (RPS) parallel mechanism in series with a THK rail mounted roller. This roller is powered by a Dynamixel AX-12A servomotor, while the parallel mechanism employs three Firgelli L12-30-210-6-P linear actuators. The position along the rail is measured using a linear potentiometer attached to the rail and has currently been calibrated to an accuracy of 1°. Feedback from the parallel mechanism is provided by built in potentiometers within the linear actuators, which have a rated accuracy of 0.2 mm. Above the eye, but connected to the frame, the single Point Grey Blackfly U3-13S2M-CS camera visual system tracks tool motion and relays coordinates for waypoint placement during the operation.

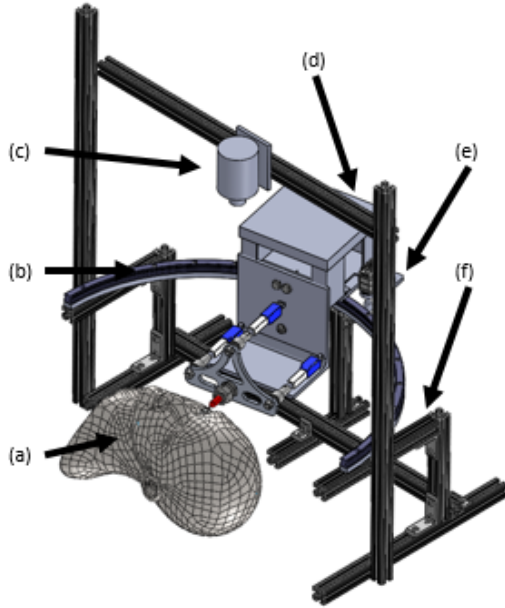


**Figure 1:** (a) Modeled Head, (b) THK Guide Rail, (c) Point Grey Blackfly U3-13S2M-CS, (d) Enclosure for Control Boards, (e) Dynamixel AX-12A, (f) Support Frame.

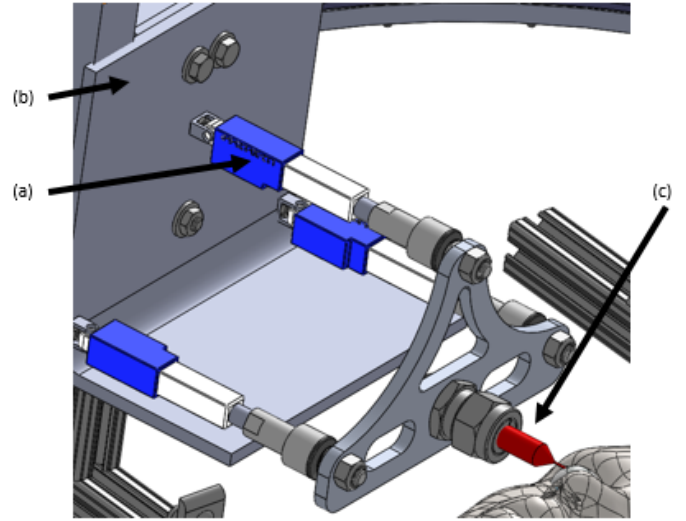


**Figure 2:** Full model of the proposed surgical platform including the curvilinear guide rail and parallel mechanism. (a) Firgelli L12 Actuators (b) Firgelli Support Plate, (c) Surgical Tool

#### B. Kinematic Analysis

To address the kinematic analysis and workspace, the coordinate frames and lengths were defined based on geometric constraints. The six frames defined for the device can be seen in Fig. 3 placing the guide rail frame directly above the eye frame and below the vision system. While computing the inverse kinematics, priority is given to the parallel mechanism due to the higher expected accuracy. Examination of the relative position of frame A to frame B therefore must give 0 in both the x and z coordinates. Should this be true, a determination of the distance required for the actuators to travel is computed. Should the extension and uncertainty be within bounds, the motion is then executed.

Forward Kinematics analysis determines the location of the tool tip for a given actuation of the robot's motors. This begins with the three linear actuator extensions  $\rho_1$ ,  $\rho_2$ , and  $\rho_3$ , as well as the angle describing the position of the roller with respect to the center of curvature of the track,  $\phi$ . To begin, the location of the tool tip  $T$  is determined with respect to the  $B$  frame. The location of the end position of actuator one, point  $a_1$ , may be written using the equation

$$\rho_1^2 = (x_{a1} - x_{b1})^2 + (y_{a1} - y_{b1})^2. \quad (1)$$

There is no z term due to the fact that  $z_{a1} = z_{b1}$ , as the actuator rotates about the z-axis. Similarly, the locations of points  $a_2$  and  $a_3$  may be expressed as

$$\rho_2^2 = (y_{a2} - y_{b2})^2 + (z_{a2} - z_{b2})^2 \quad (2)$$

$$\rho_3^2 = (x_{a3} - x_{b3})^2 + (y_{a3} - y_{b3})^2. \quad (3)$$

As with Equation 1 the x terms are excluded from equation 2 as  $x_{a2} = x_{b2}$ , and the z terms are excluded from Equation 3 as  $z_{a3} = z_{b3}$ .

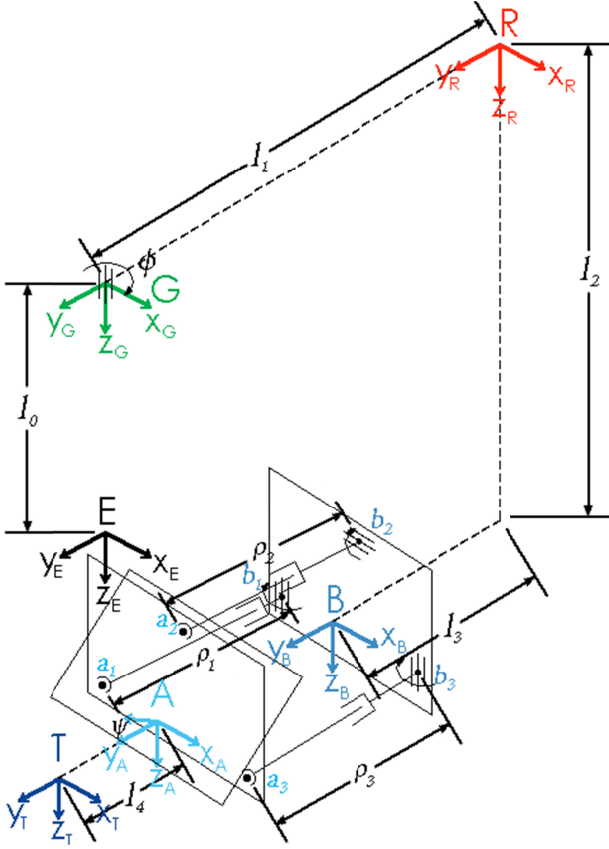


**Figure 3:** The frame locations for the system can be seen here, defining the guide rail (G), roller frame (R), fore (A) and rear (B) plates to the parallel mechanism, tool tip (T), and eye (E).

Since the distance from the origin of  $B$  to the actuator connections of  $B$  are fixed, all of the  $b_i$  coordinates are known within the  $B$  frame. Thus, there are 6 total unknowns in the systems of equations described by equations (1)-(3):  $x_{a1}, z_{a2}, x_{a3}, y_{a1}, y_{a2}$ , and  $y_{a3}$ . In order to determine a unique solution, three additional equations are required. While the exact locations of  $a_1, a_2$ , and  $a_3$  with respect to the  $B$  frame are not known, the distance from one  $a_i$  value to another is fixed. That is, the values  $|a_1 a_2|$ ,  $|a_1 a_3|$ , and  $|a_2 a_3|$  are known as these points are rigidly connected to the moving plate. Applying this to the geometry results in three additional position equations:

$$|a_1 a_2|^2 = (x_{a1} - x_{a2})^2 + (y_{a1} - y_{a2})^2 + (z_{a1} - z_{a2})^2 \quad (4)$$

$$|a_1 a_3|^2 = (x_{a1} - x_{a3})^2 + (y_{a1} - y_{a3})^2 \quad (5)$$

$$|a_2 a_3|^2 = (x_{a2} - x_{a3})^2 + (y_{a2} - y_{a3})^2 + (z_{a2} - z_{a3})^2. \quad (6)$$

The  $z$  term is excluded from equation 5, as points  $a_1$  and  $a_3$  are required to have the same  $z$  position.

As all of the equations are nonlinear, a numerical solver is used to determine the solution to equations 1-6 and provide the

coordinates of  $a_1, a_2$ , and  $a_3$  in the  $B$  frame. As the tool is rigidly fixed to the actuated plate its location within the  $A$  frame is known, and it may be located in  $B$  once the location and orientation of  $A$  are known. The angular position of the roller may then be used to create the transformation matrix between  $B$  and the eye frame  $E$ , and so fix the location of the tool tip with respect to the eye.

Global positioning allows 120 degrees of movement around the head of the patient followed by localized angular positioning of 38 degrees in the eye. Linear positioning shows extension in and out of the eye as well as a sweeping motion of approximately  $\pm 25$  mm at the eye's center, which is more than enough to cover the 12 mm diameter of an average cornea. This may be seen visually in Figure 4(a), with the base of the cornea depicted by the red circle. This setup allows the robot much more motion than required in the  $x$  direction. Decreasing this range by reducing the range of the linear actuators would unacceptably limit travel in the  $y$  direction, however. Similarly, the range of motion in the  $z$  direction spans far outside the bounds of the requirements, reaching  $\pm 5$  mm, as may be seen in Fig. 4(b). In the interest of patient safety, the device will be programmatically limited to move only within the corneal area of the eye.

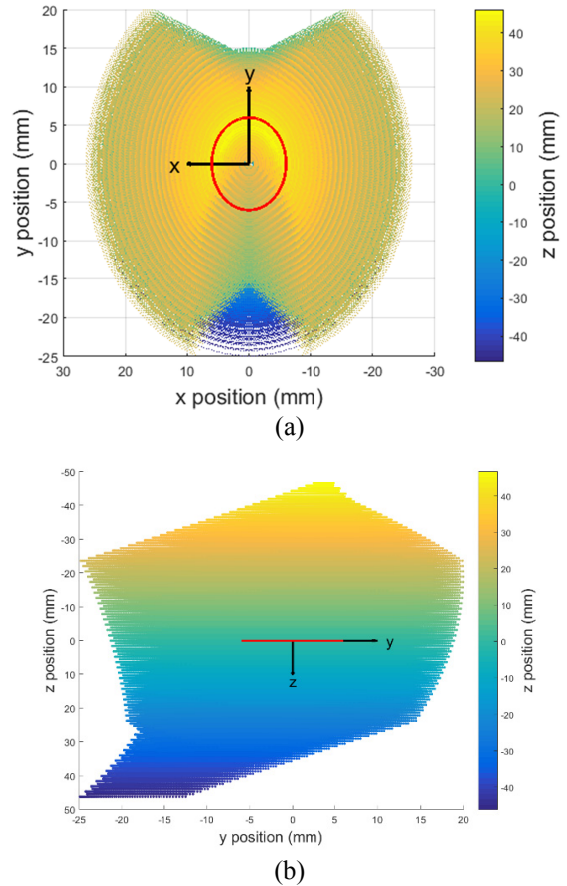


**Figure 4:** Top (a) and side (b) views of the robot's workspace. The red ring in the images represents the approximate size and location of the base of the cornea.

### C. Motor Control

To control the actuators, 4 motor control boards have been selected. The main controller is the ArbotiX-M controller used to control Dynamixel motors which will be used to control the AX-12A. This controller also functions as a standalone microcontroller. Because of this, the ArbotiX-M will control the linear actuator boards that will be used to control the Firgelli L12 linear actuators. Gain values to the control boards can be programmatically or manually set to minimize overshoot, at the cost of speed.

### D. Camera Input

In deciding upon the visual system requirements, preliminary design attempted extraction of details during surgeries, obtained through Dr. Wood. Two main goals are the segmentation of the tool from the eye during surgery followed by further extraction of the eye's current state in the surgery and the tool's identity and vector heading. Use of these details allows for motion feedback in addition to path planning each step of the operation.

Use of the surgery footage gave insights as to the use of Scale Invariant Feature Transform (SIFT) method for tool identification through a Support Vector Machine (SVM). At a word count of 800, three tools were attempted for identification: the keratome blade seen in Figure 5, forceps, and a phacoemulsification probe. Manual entry of descriptors were entered for  $N=17\pm 1$  then exposed to  $N=1500\pm 100$  images from throughout the surgery in attempts to localize frames containing the tool. Through this, issues such as tool reflection, low signal to noise ratio (SNR), and lack of descriptor relative position to each other gave high false positives.

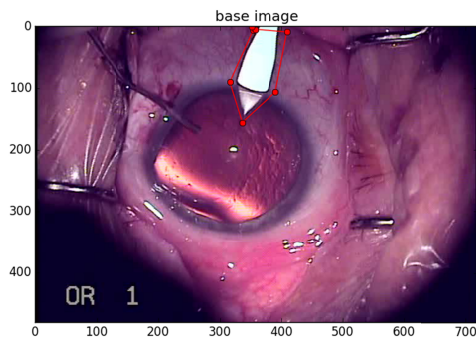


**Figure 5:** Manual descriptor entry for various surgical tools under surgical settings gave low matching scores using SIFT. Reflections, low SNR, and lack of descriptor relative positions revealed many issues in implementation.

This led to the current assessment of contour and texture containing the most robust information and absolute importance of high streaming quality. Limiting the workspace to 88 by 66 mm and requiring details of 0.1 mm to be visible, a 1288 by 964 monochrome, 25 FPS, 12-bit camera and 35 mm lens system to be selected for a working distance of 640 mm. Scenarios where this submillimeter accuracy will be necessary

include finding the entry incision for tool re-insertion, tool monitoring, and accurately assessing where the procedure should take place.

### D. System Tolerances and Accuracy

In order to determine the required accuracy and non-obvious considerations for the robot, we consulted with Dr. John Wood. The initial incision into the eye, the scleral tunnel, requires an accuracy of 0.5 mm in the length of the cut. Furthermore, no part of the robot may come in contact with the posterior of the capsule holding the lens or the underside of the cornea without risking complications to the surgery. The requirements translate to required tool position accuracies of 1.77 mm in the x and y directions in the horizontal plane, as well as an accuracy of 1.139 mm in the vertical z direction.

As mentioned previously, the Firgelli linear actuators have a stated accuracy of 0.2 mm. By utilizing the sequential perturbation method, the expected tool positioning errors in the x, y, and z directions are 0.167 mm, 0.141 mm, and 0.290 mm, respectively. It should be noted that these values neglect errors in the physical geometry of the robot, as it is expected that these uncertainties will be removed with proper calibration. Further, the projected error in the x, y, and z coordinates of the tool were calculated using the sequential perturbation method due to the numerical nature of the forward kinematics calculation, and are therefore not exact. Given that these errors are almost an order of magnitude within tolerance, however, it is expected that the system will be able to achieve the required accuracy.

The accuracy of the rotation about the rail has currently been performed to  $1^\circ$ , which provides a maximum error in the length of the scleral tunnel of 0.1047 mm. The resistance measured from the potentiometer was found to be linear across its entire range, and as such the accuracy is expected to be higher than this value. The hysteresis of the potentiometer has not yet been examined, however, and geometric errors are neglected as they were for the parallel mechanism. Utilization of the overhead camera for tool position feedback, in addition to its path planning, gives additional compensation for drift or inaccuracies in the system. At a working distance of 640 mm and angular field of view of  $7.4^\circ$ , the Point Grey Blackfly can expect nearly 14.6 pixels of coverage for every millimeter. The workspace given by such a configuration gives an area of 88 mm by 66mm, covering the entire eye and tool entry location. Operating at 25 frames per second with a global shutter, the location of the tool would be within 0.08 mm every frame at a speed of 2 mm/s.

## IV. CONCLUSIONS AND FUTURE WORK

### A. Summary

In summary, the system described in this paper is a proof of concept and the beginnings of a platform that would perform autonomous cataract surgery. Workspace analysis shows that the current design can reach all parts of the eye needed to perform the simplified surgical procedure. A semi-circular

guide rail, providing 120 degrees of movement around the head and 38 degrees in the eye, affords ample room for the minimum expected procedure. Full extension and retraction of  $\pm 25$  mm at the eye's center provides enough to cover the 12mm diameter of an average cornea. Through the nature of the parallel mechanism, a z-axis extension of  $\pm 25$  mm from the center of the eye without requiring full joint extension. in the x, y, and z directions are 0.167 mm, 0.141 mm, and 0.290 mm, respectively, falling within surgeons' acceptable ranges. An error of 0.1047 mm in the length of the scleral tunnel is expected. Limitations on speed are constrained by the vision system, requiring no faster than 2 mm/s to maintain visual contact between frames in intervals of 0.08 mm at 25 frames per second. Mechanical and system design has been completed and construction is underway. Considerations for power draw from a standard 120VAC source give full operation even at stall current at all actuators. Next steps towards completion of the project include computing the inverse kinematics, communicating between different systems, and controlling motors. Such framework will be handled mainly by ROS and associated modules in association with Python and OpenCV Libraries.

#### B. Future Work

Upon the arrival of parts, the subsystems will be assembled, tested, and then integrated into a final assembly. One hurdle in maintaining accuracy is ensuring a no-slip condition between the rail and Dynamixel Servo-drive with functional linear potentiometer. Another is the perfect alignment of all Firgelli linear actuators with the base plate and tool holster. Calibration of the actuations in synchronization will need to take place in conjunction with parallel work in the camera and lighting system.

In a study approved by the Virginia Tech Institutional Review Board, preliminary data on clouding of the lens in human eyes was collected. The study procedure included imaging of healthy, post-surgery, and pre-surgery eyes. Due to lack of proper optics and lighting capable of producing a red-reflex, information obtained thus far was limited. Use of an ophthalmoscope in conjunction with the Blackfly camera should overcome these limitations for illuminating the fundus, as in an eye exam. Information from such trials will assist in the development of more exact test eyes' variation between patients. Additional data has been obtained from Dr. Wood's own surgeries, albeit performing the surgery with a phacoemulsification probe.

Once fully assembled, tests will be developed to test the design of the system's accuracy and feasibility. Development of the ROS based software architecture through Python and computer vision detection and trajectory planning will follow as well. Testing with the system relies on ballistics gel constructed mannequin eyes. With all components completed, a simulated surgery may be tested and improved upon. Beyond these goals, eventual integration of additional degrees of

freedom would allow more delicate aspects of the full procedure to be carried out.

#### ACKNOWLEDGMENTS

We wish to thank Dr. John Wood, MD, Vistar Eye Center, Salem, VA for his support and invaluable advise on this Senior Design Project.

We would also like to thank Jason Ziglar for his advice and assistance in learning and setting up the ROS framework, and John Seminatore for his help with the detailed mechanical design and applied robotics knowledge.

#### REFERENCES

- [1] Foster, A., 2000. "Vision 2020: The Cataract Challenge". *Community Eye Health*, 13(34), pp 17–19.
- [2] Jadoon, A., Shah, S. P., Bourne, R., Dineen, B., Khan, M. A., Gilbert, C. E., Foster, A., Khan, M. D., 2007. "Cataract prevalence, cataract surgical coverage and barriers to uptake of cataract surgical services in Pakistan: the Pakistan National Blindness and Visual Impairment Survey". *Br J Ophthalmol*, 91(10), pp 1269–1273.
- [3] Thylefors, B., Negrel, A. D., Parajasegaram, R., Dadzie, K. Y., 1995. "Global data on blindness". *Bull World Health Organ*, 73(1), pp 115–121.
- [4] Allen, D. 2006. "Cataract and surgery for cataract". *BMJ*, 333(7559), pp 128–132.
- [5] Beasley R. A., 2012. "Medical Robots: Current Systems and Research Directions". *Journal of Robotics*, 2012(2012), Article ID 401613, 14 pages.
- [6] Vasilescu, D., 2012. "Surgical treatment of parietal defects with "da Vinci" surgical robot". *J Med Life*, 5(2): pp 232–238.
- [7] Kehoe, B., Kahn, G., Mahler, J., Kim, J., Lee, A., Lee, A., Nakagawa, K., Patil, S., Boyd, D. W., Abbeel, P., Goldberg, K. 2014. "Autonomous Multilateral Debridement with the Raven Surgical Robot". *Robotics and Automation (ICRA), 2014 IEEE International Conference*, pp 1432 – 1439
- [8] Moustiris, G. P., Hirisidis, S. C., Deliparaschos, K. M., Konstantinidis, K. M., 2011. "Evolution of autonomous and semi-autonomous robotic surgical systems: a review of the literature". *International Journal of Medical Robotics and Computer Assisted Surgery*, 7(4), pp. 375–392.
- [9] Mayer, H., Nagy, I., Knoll, A., Braun, E. U., Lange, R., Bauernschmitt, R., 2007. "Adaptive Control for Human-Robot Skill Transfer: Trajectory Planning Based on Fluid Dynamics". *Robotics and Automation*, (ICRA), 2007 IEEE International Conference, pp 1800-1807.
- [10] Rahimy, E., Wilson, J., Tsao, T. C., Schwartz, S., Hubschman, J-P., 2013. "Robot-assisted intraocular surgery: development of the IRISS and feasibility studies in an animal model". *Eye*, 27, pp 972–978.
- [11] Gillies, M., Brian, G., Nauze, J. L., Mesurier, R. L., Moran, D., Taylor, H., Ruit, S., 1998. "Surgery for Global Cataract Blindness: Preliminary Considerations". *Arch Ophthalmol*, 116(1), pp 90-92.
- [12] Tsui, I., Tsirbas, A., Mango, C. W., Schwartz, S. D., Hubschman, J., 2010, "Robotic Surgery in Ophthalmology", *Robot Surgery*, Chapter 10.